Integral Equation Methods in the Computation of Equilibrium Properties of Ionic Solutions*

JAYENDRAN C. RASAIAH AND HAROLD L. FRIEDMAN

Department of Chemistry, State University of New York, Stony Brook, New York

(Received 18 September 1967)

Computations have been made for a system of charged hard spheres with parameters chosen to correspond to an aqueous solution of a 1–1 electrolyte in the range from 0.001 to 1M. Correlation functions were computed by the analogues of the HNC and PY integral equations due to Allnatt in which the integral equations are constructed after the Mayer resummation has been performed on the expansion of $g(r)$. Activity and osmotic coefficients are computed both by the compressibility and pressure equations and tested for consistency. Based on this test and others, including a comparison with computations published by Carley, it is concluded that the HNC equation gives very accurate results for this primitive model at least up to 1M. The accurate results show that the effect of the excluded volume of the hard-sphere cores has been considerably underestimated in earlier treatments of the primitive model.

I. INTRODUCTION

The objective of the work described here is to treat the simplest model of an electrolyte solution with sufficient accuracy so that over a substantial composition range the thermodynamic properties of a hypothetical system constructed according to the model will be known within limits that are small compared to the experimental uncertainty in the best measurements on the corresponding real physical systems. While this is not asking much compared to the magnitude of the problem of achieving an understanding of the real systems on a molecular level, it may not be an insignificant contribution to a field in which the theoretical contribution of towering importance is only asymptotically valid in the limit of zero concentration of the ions.

Our efforts toward this objective have been spurred by the fact that the underlying theory and computational methods are now available, having been developed in applications to simpler systems. The theoretical framework we used is an adaptation by Allnatt[1] of the integral equation methods that have mostly been employed in the calculation of the thermodynamic properties of one-component gases at densities up to the critical. The same methods have recently been applied more directly to this problem by Carley[2] while the Monte Carlo method, which has also been developed for computations with simple gases and fluids, has been applied by Brush, Sahlin, and Teller[3] only to the model of point charges of one sign in a uniform background of the other. We make some comparison of our results with Carley's in the concluding section of this paper.

The main importance of the present work lies in the fact that unless the simplest models are treated exactly, the difference between the deductions from the model and the behavior of experimental systems may lead to wrong conclusions about the sort of elaboration of the model needed for more faithful representation of the real system. This homily has been demonstrated often enough in the history of the electrolyte solution field but even so there are indications in the present work that still another example is upon us.

Because of the validity of the McMillan–Mayer theory[4] an expression for the pressure P of a gas as a functional of the intermolecular pair potential $u_{ij}(r)$ also gives the osmotic pressure of a solution as the *same functional* of a certain pair potential function $u_{ij}^0(r)$ of the solute molecules. The $u_{ij}^0(r)$, often called the potential of average force at infinite dilution, is the potential of the force acting between i and j maintained at the distance r apart in the *pure* solvent. We shall take advantage of the McMillan–Mayer theory to switch back and forth between gas-like and solution-like terminology according to what is simplest and clearest. In particular we use the same notation P for the pressure of the gas or the osmotic pressure of the solution and shall use the same name, the *direct potential*, and the same notation, u_{ij}, for either u_{ij} in the gas or u_{ij}^0 in the solution. Similarly the correlation function $g_{ij}(r)$ may be the correlation of either the arbitrary pair of molecules i and j in the gas or the pair of solute molecules i and j in the solution; also for this the McMillan–Mayer theory shows that the functional dependence on the direct potential is the same in either case.

Now we are concerned with a system containing c_1 ions per unit volume of species 1, c_2 of species 2, $\cdots$, and finally c_σ of species σ. The direct potentials may be written

$$u_{ij}(r) = u_{ij}^*(r) + e_i e_j/\epsilon r, \tag{1.1}$$

where ϵ is the dielectric constant of the medium (the

* Research supported by Office of Saline Water.

[1] A. R. Allnatt, Mol. Phys. **8**, 533 (1964).

[2] D. D. Carley, J. Chem. Phys. **46**, 3783 (1967).

[3] S. G. Brush, H. L. Sahlin, and E. Teller, J. Chem. Phys. **45**, 2102 (1966).

[4] W. G. McMillan and J. E. Mayer, J. Chem. Phys. **13**, 276 (1945).

vacuum for a gas or the pure solvent for a solution). We assume that the potential energy of an assembly of any number of ions at fixed locations can be computed by summing over the direct pair potentials u_{ij}. We also assume that the non-Coulomb term u_{ij}^* is the hard-sphere potential

$$u_{ij}^*(r)=\infty \quad \text{if} \quad r<a_{ij}$$
$$=0 \quad \text{if} \quad a_{ij}<r, \tag{1.2}$$

where the a_{ij} are parameters of the model. The first assumption is essential for the computations we make while the second can be replaced with others with only minor changes in the program.

The basic theory for our work is Mayer's expansion[5,6] for the excess Helmholtz free energy per unit volume F^{ex},

$$-F^{ex}/kT=(\kappa^3/12\pi)+\sum_{n\geq 2} c^n B_n(\kappa), \tag{1.3}$$

where n is a set of ions; we sum over all sets of two or more ions, where

$$c^n \equiv c_1^{n_1} c_2^{n_2} \cdots,$$

where

$$\kappa^2 \equiv 4\pi \sum_{i=1}^{\sigma} c_i e_i^2/\epsilon kT \tag{1.4}$$

and where the $B_n(\kappa)$ are similar to the virial coefficients B_n in the virial expansion of F^{ex} or P for a system of neutral molecules. The principle difference is that wherever u_{ij} appears in B_n we have instead

$$u_{ij}'=u_{ij}^*+e_i e_j e^{-\kappa r}/\epsilon r \tag{1.5}$$

in $B_n(\kappa)$. As a result whereas the topological description of B_n is in terms of Mayer f bonds,

$$f_{ij} \equiv \exp(-u_{ij}/kT)-1, \tag{1.6}$$

the topological description of $B_n(\kappa)$ is in terms of q bonds

$$q_{ij} \equiv e_i e_j e^{-\kappa r}/\epsilon r kT \tag{1.7}$$

and Φ'' bonds

$$\Phi_{ij}'' \equiv [1+k_{ij}] \exp(q_{ij})-1-q_{ij}, \tag{1.8}$$

where k_{ij} is defined by

$$k_{ij} \equiv \exp(-u_{ij}^*/kT)-1. \tag{1.9}$$

The term $\kappa^3/12\pi$ in Eq. (1.4) is the Debye–Hückel limiting law (DHLL) for this function. An approximation to F^{ex} that is equivalent in accuracy with a number of other widely-used approximations is

$$-F^{ex}/kT=(\kappa^3/12\pi)+\sum_{i=1}^{\sigma}\sum_{j=1}^{\sigma} c_i c_j B_{ij}(\kappa). \tag{1.10}$$

This and the corresponding approximations for other thermodynamic functions are easy to evaluate; we shall designate them DHLL+B_2 approximations and make some use of them to represent the rather widespread notion of the exact behavior of the primitive model treated here. These approximations are also useful in the simplification of certain computations. Tables of the DHLL+B_2 approximations were first given by Poirier[7]; others have been given by Friedman,[6] but it is easiest to evaluate DHLL+B_2 by a simple computer program using the expressions in closed form for this approximation derived by Meeron.[8]

II. THE INTEGRAL EQUATIONS

The theory of the integral equations we solve has been worked out by Allnatt.[1] The derivation is outlined here to make the significance of the various functions clear.

The pair correlation function for ions i and j may be written in the form

$$g_{ij}=(1+k_{ij}) \exp(q_{ij}+\alpha_{ij}). \tag{2.1}$$

If we suppress α_{ij} and linearize the exponential we have the Debye–Hückel correlation function. Meeron[9] has shown from Mayer's ionic solution theory that α_{ij} has the cluster expansion

$$\alpha_{ij}=\sum_{m\geq 1} \frac{c^m}{m!} \int Q(ij:m)\, d\{m\}, \tag{2.2}$$

where $m! \equiv m_1! m_2! \cdots m_\sigma!$

The integrand $Q(ij:m)$ is a sum of terms, each of which is a product of certain functions. The product may be represented as a graph on two root points, corresponding to ions i and j, and m field points, corresponding to m other ions. These points are connected by lines (bonds) corresponding to the factors in the product. The allowed bonds are either q bonds, or Φ'' bonds, and the integration of $Q(ij:m)$ is over the coordinates $\{m\}$ of the field points.

Among the terms of $Q(ij:m)$ is every product which may be represented by a graph with the following characteristics:

(a) Every vertex of m is connected to both i and j by independent paths.

(b) All field points of m are connected amongst themselves independent of i and j.

(c) There are no field points connected to the rest of the graph only by two q bonds.

A few examples are shown in Fig. 1.

When one examines this graphical representation of the terms of α_{ij} he sees that there is a redundancy that

[5] J. E. Mayer, J. Chem. Phys. **18**, 1426 (1950).
[6] H. L. Friedman, *Ionic Solution Theory* (Interscience Publishers, Inc., New York, 1962).
[7] J. C. Poirier, J. Chem. Phys. **21**, 965 (1953).
[8] E. Meeron, J. Chem. Phys. **26**, 804 (1957).
[9] E. Meeron, J. Chem. Phys. **28**, 630 (1958).

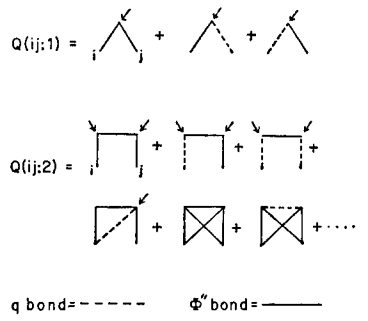

FIG. 1. Some cluster diagrams for α_{ij}. The complete set is shown for $Q(ij:1)$, but only a few for $Q(ij:2)$ are shown. Cutting points are indicated by arrows.

enables it to be put in another form. To see this we write

$$\alpha_{ij}=\tau_{ij}+\zeta_{ij}, \tag{2.3}$$

where τ_{ij} is the sum of all the terms of Eq. (2.2) in which the graphs have *cutting points* and ζ_{ij} is the remainder. Cutting points are field points at which the graph may be cut into two disconnected parts. Examples are designated by arrows in Fig. 1. Except for $Q(ij:1)$ which contributes only to τ_{ij}, all the $Q(ij:m)$ contribute some terms to τ_{ij} and some to ζ_{ij}.

Any one of the terms of τ_{ij} may be written as

$$\sum_{k=1}^{\sigma} c_k \int \theta_{ik} d\{1_k\} \psi_{kj} \equiv \theta_{ik} * \psi_{kj}, \tag{2.4}$$

where k is the species of the molecule at the cutting point nearest to i, and $\{1_k\}$ its coordinate. The special notation $*$ here indicates we sum over the species at the cutting point and do the convolution integral. A still more compact notation for this term is

$$\theta * \Psi,$$

which represents the σ^2 terms obtained from (2.4) by letting i and j be each pair of species in turn. The analogy to a matrix representation is obvious, and we use it below with the understanding that the operation $*$ is defined by Eq. (2.4).

We now obtain an expression for τ. Let X_{kl} be the sum of all diagrams which may be found connecting two adjacent cutting points k and l of τ_{ij}, except that the single q_{kl} bond is excluded.

Then, in matrix notation, we have

$$X=h-q-\tau, \tag{2.5}$$

where h_{ij} is defined by

$$h_{ij}=g_{ij}-1 \tag{2.6}$$

and we see that g_{ij} appears in its own cluster expansion which is the basis of the integral equations which follow. We may also write

$$\tau=A+B, \tag{2.7}$$

where B_{ij} is the collection of all of the terms in τ_{ij} in which the bond connecting i to the nearest cutting point is a q bond, while A_{ij} is the remainder. Hence

$$B=q*(A+X) \tag{2.8}$$

and

$$A=X*(q+X+\tau)$$
$$=X*h. \tag{2.9}$$

If we now combine Eq. (2.7), (2.8), and (2.9) we have

$$\tau=X*h+q*X+q*X*h. \tag{2.10}$$

Allnatt's integral equation is found by substituting Eq. (2.5) in (2.10) and then eliminating τ by use of Eq. (2.1):

$$\ln(1+h_{ij})=\ln(1+k_{ij})+q_{ij}+\tau_{ij}+\zeta_{ij}. \tag{2.11}$$

Now only q and k are known and we have only one equation to solve for both h and ζ unless there is further information. As suggested by Allnatt,[1] we employ two approximations for the missing information:

The analog of the hypernetted-chain equation: Approximate Eq. (2.11) by

$$\ln(1+h_{ij})=\ln(1+k_{ij})+q_{ij}+\tau_{ij}. \tag{2.12}$$

The analog of the Percus–Yevick equation: Approximate Eq. (2.11) by

$$\ln(1+h_{ij})=\ln(1+k_{ij})+q_{ij}+\ln(1+\tau_{ij}). \tag{2.13}$$

It would of course be of interest to extend these results to the analogs of the self-consistent approximations of Hurst[10] and Rowlinson[11] and others, but it seems unlikely that this would change the general character of our conclusions.

We have in fact considered three simpler approximations which do not even involve integral equations. The first of these is the approximation

$$\ln(1+h_{ij})=\ln(1+k_{ij})+q_{ij} \tag{2.14}$$

and the others are the $\omega(\Lambda)$ approximation

$$\ln(1+h_{ij})=\ln(1+k_{ij})+q_{ij}+\sum_{k=1}^{\sigma} c_k \int Q(ij:1_k) d\{1_k\} \tag{2.15}$$

and the $g(\Lambda)$ approximation

$$\ln(1+h_{ij})=\ln(1+k_{ij})+g_{ij}$$
$$+\ln[1+\sum_{k=1}^{\sigma} c_k \int Q(ij:1_k) d\{1_k\}]. \tag{2.16}$$

Equation (2.14) retains only the leading term $(-u^*/kT+q)$ in the potential of average force, while the $\omega(\Lambda)$ approximation corrects this to the extent of adding the first term in the cluster expansion of α_{ij}, and the $g(\Lambda)$ approximation similarly corrects the pair-correlation function. Of the three, the results of

[10] C. Hurst. Proc. Phys. Soc. (London) **86**, 193 (1965).
[11] J. S. Rowlinson, Mol. Phys. **9**, 217 (1965).

the $g(\Lambda)$ approximation lie closest to the solutions of the HNC and PY equations.

To solve these integral equations we begin conveniently with the $g(\Lambda)$ approximation. The sum

$$\sum_k c_k \int Q(ij:1_k)\,d\{1_k\}$$

is the ij element of the lowest-order approximation to τ, call it τ_0. Equation (2.16) now yields a low-order approximation to h, call it h_0. The next step is to solve for X_0 using Eq. (2.5). The sets of functions h_0, X_0 are now substituted on the right of Eq. (2.10) which is evaluated to get the first refined value of τ, call it τ_1. The procedure begun with τ_0 is now repeated using either Eq. (2.12) or (2.13) in place of Eq. (2.16) as appropriate, to solve for h in each iteration until the functions no longer change when the cycle is repeated.

When the right side of Eq. (2.10) is to be evaluated, for example in getting τ_1, we proceed by Fourier transformation and the use of the convolution theorem which gives an equation of the same form as Eq. (2.10) except that in place of each function f_{ij} we have its Fourier transform $\tilde{f}_{ij}$ and in place of the operation $f*F$ we have the matrix multiplication

$$\tilde{f}\cdot\mathbf{c}\cdot\tilde{F},$$

where

$$\mathbf{c}=\mathrm{diag}(c_1,\cdots,c_\sigma) \tag{2.17}$$

is the matrix of the concentrations. On completing these arithmetic operations in transform space on the right side of Eq. (2.10), the result is inverted to get τ_1 itself. The chief aspect in which this iterative procedure differs from the procedure for solving the original HNC equation by Fourier transform is in the solution of Eq. (2.10), where one now has to solve a matrix equation rather than a single algebraic equation. Except for this and the need to store more functions, the numerical procedure is not more complicated than for the one-component case because the Fourier transformations may be done seriatim.

The procedure described above, if the iteration converges, leads to the exact set h except for the approximations inherent in the HNC or PY equations. We list here four kinds of approximations which result from the numerical procedures we use:

Finite range of integration. The Fourier transformation integrals

$$\tilde{f}_{i,j}(k)=4\pi\int_0^L f_{i,j}(r)\,\sin(rk)\,(r/k)\,dr,$$

$$f_{i,j}(r)=(1/2\pi^2)\int_0^K \tilde{f}_{i,j}(k)\,\sin(rk)\,(k/r)\,dk, \tag{2.18}$$

which are properly evaluated for $L=\infty=K$, are evaluated for finite L and K instead.

Replacement of integrals by sums. The finite integrals resulting from the above approximation are each approximated as a sum over N terms.

Use of FORT. A fast numerical procedure (FORT) for evaluating these Fourier transform sums in the case $N=2^n$, where n is an integer, is applied to the present case where, for reasons described in Sec. III, it results in a certain error.

Neglect of round-off errors in the numerical procedures. As we shall see, in some cases the thermodynamic functions depend in a very sensitive way on the correlation functions so we may be concerned with rather high accuracy in these computations.

An essential part of the work reported here is the effort to evaluate the significance of each of these approximations; except for this the computation is quite straightforward. In the following sections we describe the calculations in more detail and present the principal results together with the studies of the approximations.

III. NUMERICAL SOLUTION OF THE INTEGRAL EQUATIONS FOR $g_{ij}(r)$

As Broyles[12] has shown the following discrete representation of the Fourier transforms in Eq. (2.18) preserves the reciprocity between them:

$$\begin{aligned}\tilde{f}_{i,j}(k)&=\tilde{f}_{i,j}(m\hat{k})\\&=[4\pi\hat{r}^2/m\hat{k}]\sum_{n=0}^{N-1} nf_{i,j}(n\hat{r})\,\sin(nm\hat{r}\hat{k}),\\ f_{i,j}(r)&=f_{i,j}(n\hat{r})\\&=[\hat{k}^2/2\pi^2n\hat{r}]\sum_{m=0}^{N-1} m\tilde{f}_{i,j}(m\hat{k})\,\sin(nm\hat{r}\hat{k}),\end{aligned} \tag{3.1}$$

provided that we fix

$$\hat{r}\hat{k}=2\pi/(2N-1), \tag{3.2}$$

where $\hat{r}$ is the interval in the r space and $\hat{k}$ in the k space and N is an integer. Thus the upper bounds in Eq. (2.18) are $L=(N-1)\hat{r}$ and $K=(N-1)\hat{k}$.

To evaluate the sums in Eq. (3.1) we have used the fast Fourier transform FORTRAN program called FORT[13,14] which exploits an algorithm for sums of the form

$$\bar{u}(m)=\sum_{n=0}^{M-1} u(n)\,\exp(2\pi inm/M), \tag{3.3}$$

where $M=2^l$ and l is in integer. The program enables us to recover real and imaginary parts of the functions

[12] A. A. Broyles, quoted in F. Lado, Ph.D. thesis, University of Florida (1964).

[13] FORT, IBM SHARE Distribution Agency (S.D.A.) No. 3465.

[14] J. W. Cooley and J. W. Tukey, Math. Computation 19, 297 (1965).

separately and we have, if $u(n)$ is real,

$$\mathrm{Im}\tilde{u}(m)=\sum_{n=0}^{M-1} u(n)\,\sin(2\pi nm/M), \qquad (3.4)$$

which is just of the form of the sums in Eq. (3.1) except that $M=2^l$ is even while $2N-1$ is odd, and M is the number of terms while $2N$ is twice the number of terms. What we have done to employ the FORT program is to use (3.4) with $M=2^l=2N$, and with

$$\begin{aligned} u(n)&=nf_{i,j}(n\hat{r}) \quad \text{for} \quad 0\leq n\leq N-1 \\ &=0 \qquad\quad\ \ \text{for} \quad N\leq n\leq 2N-1. \end{aligned} \qquad (3.5)$$

Then, for example, for $N=2^9=512$, we need $2^{11}=2024$ words in the computer core for the Fourier transform in the FORT operation: 512 each in the real and imaginary parts for $n<N$ and for $n>N$. This is not very efficient but it seemed advisable to proceed with the present calculation before attempting to optimize the program. The remaining difficulty, that in the argument of the sine function in Eq. (3.4) we have $M=2N$ in place of $2N-1$, causes an error of almost $1/N$ in the resulting transforms. This can be reduced by a perturbation correction but this was found not to be worthwhile. Of course the same procedure was used for the inverse transformation in Eq. (3.1).

The computations were done on an IBM 7044 computer with a core of 32 000 36-bit words and cycle time of 2-μsec. With $N=512$ the same transforms required 0.91 min by trapezoid rule computation and 0.03 min by FORT, a ratio of 30; for $N=1024$ the ratio was 60. Using $\hat{r}=0.015/\kappa$ and $N=512$, the transform of $e^{-\kappa r}/r$ obtained by trapezoid rule and FORT were compared: the results agreed everywhere within 0.1%. The forward FORT transform was inverted by FORT: the original function was recovered with an error of less than 0.05% at each value of n except $n=0$ where the error was 39%. We can neglect this apparent truncation error since $f_{i,j}(n\hat{r})$ for $n=0$ has zero as a multiplier in the summand of Eq. (3.1). There is of course also a real truncation error which is most easily investigated by reducing it by extending the range N of integration. As described below, we find that this error is negligible in the present work.

Most of the computations have been done with $\hat{r}\sim 0.015/\kappa$ where κ is the Debye–Hückel parameter. This interval has been chosen as a compromise between a longer one which extends the range of integration and a shorter one which gives a greater density of sampling points which is helpful for $r\sim a$. We find this compromise together with $N=512$ to be satisfactory for 1–1 electrolytes in water but not for 2–2 electrolytes in water. In the latter case a larger N is necessary. The exact value of $\hat{r}$ must be chosen so that in transforming any $f(n\hat{r})$ there is a sampling point $n\hat{r}$ at a_{ij}, the repulsive core diameter, for each of the pairs $ij=++$, $+-$, and $--$. Clearly this puts a restriction on the way the set of a_{ij} is chosen but it is not very serious with N as large as 512. The program is written to accomodate more complicated direct potentials than hard-sphere plus Coulomb, but its use with more complicated potentials requires that N be large enough so that one can have a high density of sampling points wherever there are features of interest in the direct potential while maintaining a range of integration as large as that used in the present work, namely $L=511\times 0.015/\kappa$. In these solutions κ^{-1} varies from 96 Å at $0.001M$ to 3 Å at $1M$.

The trial function, τ_0, is evaluated by computing the $Q(ij:1_k)$ integrals. We have

$$\begin{aligned} (\tau_0)_{ij}&=\sum_{k=1}^{\sigma} c_k \int Q(ij:1_k)\,d\{1_k\} \\ &=\Phi_{ik}'*\Phi_{kj}'-q_{ik}*q_{kj} \\ &=\Phi_{ik}'*\Phi_{kj}'+\tfrac{1}{2}(q_{ij}r_{ij}\kappa), \end{aligned} \qquad (3.6)$$

where the second term has been evaluated analytically, and the Φ' bond is defined by

$$\Phi_{ij}'\equiv\Phi_{ij}''+q_{ij}. \qquad (3.7)$$

The first term in Eq. (3.6) is calculated by Fourier transformation using the numerical technique we have just described, and the convolution theorem.

The convergence of the iteration process was followed by observing the behavior of the thermodynamic function $d\ln\gamma_{\pm}/dc_2$ which was computed at various stages of the iteration by the procedure described in the following section.[15] The iteration was stopped when $d\ln\gamma_{\pm}/dc_2$ remained constant within 0.001%. This convergence is shown for four typical cases in Table I. It will be noted that we did not find it necessary to use any tricks to get this rapid convergence when the trial function was chosen as described above. Convergence difficulties were encountered when the program was applied to parameters appropriate to 2–2 electrolytes in water at 25° unless the molarity was larger than $0.1M$. It seems that 512 sampling points is not enough for such a steeply varying potential as we get here when κ is small; under these circumstances it does not seem worthwhile to force convergence by some sort of trick.

A family of correlation functions computed by the HNC equation is shown in Fig. 2. They are all qualitatively similar to each other and similar as well to the results of the PY equation and to the results obtained from both equations by Carley.[2] Even choosing a_{++}, a_{+-}, and a_{--} all different from each other does not appear to do more than shift the curves along the r axis.

[15] This requires between three and five times the number of iterations for the convergence of the osmotic coefficient ϕ since, as shown in Sec. IV, it is related to the first moment of g_{ij}, while $\partial\ln\gamma_{\pm}/\partial c_2$ is related to the second moment of this function.

TABLE I. Convergence of the iterative process for the HNC equation. $a_{++}=a_{--}=a_{+-}=4.6$ Å.

Molarity	Percent difference in $d\ln\gamma_\pm/dc_2$ from the final value of the HNC equation for the following number of iterations: 0	5	6	8	10	11	15	16	$d\ln\gamma_\pm/dc_2$ From trial function g_{ij} (A)	Final value (HNC eq.)
0.001	−0.420	0.000	0.000						−16.59	−16.66
0.1	0.974	−0.095	0.000	0.000					−0.4248	−0.4247
0.5	3.780	−0.996			0.000	0.000			0.3019	0.2909
0.9[a]	−1.557	−5.980			−0.226		0.023	0.000	0.4362	0.4431

[a] Final value after 20 iterations.

It is of interest to find whether $g_{ij}=g_{ji}$ when $i\neq j$ for the computed functions. Although this equality obtains in principle, some steps of the computation of the integral equations do not appear to be identically symmetrical in the interchange of the particles i and j, and we were quite prepared to find it necessary to insert a symmetrizing step in the iteration chain. One test for this consistency is to calculate, for the system with asymmetrical ion sizes, the quantities G_{ij} and G_{ji} where $i\neq j$ and G_{ij} is defined in Eq. (4.9) of Sec. IV. We find that $G_{ij}=G_{ji}$ to within 0.01% at each concentration for which solutions were obtained to the HNC and PY equations. Thus we have no reason to doubt the symmetry of the computed correlation functions.

IV. COMPUTATION OF THERMODYNAMIC FUNCTIONS FROM $g_{ij}(r)$

We have computed the excess free-energy functions from the pair correlation functions using the generalizations to ionic solutions of the following equations for one component systems: the pressure equation

$$\frac{P^{ex}}{ckT}=\frac{P}{ckT}-1=-\frac{c}{6kT}\int_0^\infty r\frac{\partial u}{\partial r}g(r)4\pi r^2dr \quad (4.1)$$

and the compressibility equation

$$(kT)^{-1}(\partial P^{ex}/\partial c)_T=-Gc/(1+Gc), \quad (4.2)$$

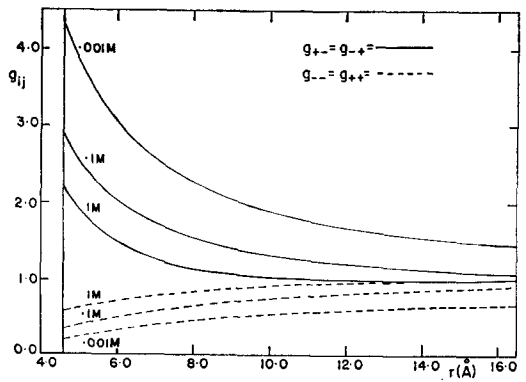

FIG. 2. Correlation functions $g_{ij}(r)$ obtained from the HNC approximation at $I=0.001$, 0.1, and $1M$ for a 1–1 electrolyte in H_2O at 25°C assuming $a_{++}=a_{--}=a_{+-}=4.6$ Å. I is the molar ionic strength.

where

$$G=\int_0^\infty h(r)4\pi r^2dr$$

and c is the number density of the one-component system. In addition a third method, the use of the familiar charging parameter, was considered but not used here since it requires solutions of the integral equations for many values of this parameter at each concentration of interest and does not seem to offer any compensating advantage.

The generalization of Eq. (4.1) to multicomponent systems is well known. If the direct potential is pairwise additive, as in the model treated in this paper, it is

$$P-ckT\equiv P^{ex}$$
$$=-\tfrac{1}{6}\sum_{i=1}^{\sigma}\sum_{j=1}^{\sigma}c_ic_j\int_0^\infty r\frac{\partial u_{ij}}{\partial r}g_{ij}(r)4\pi r^2dr, \quad (4.3)$$

where now c is the sum of the particle number densities of the solute species in the case of a solution or all species in the case of a gas, and P^{ex} is the excess osmotic pressure in the first case and the total excess pressure in the second. In the former case this P^{ex}/ckT is the same as $\phi-1$ where ϕ is the osmotic coefficient for a system in which the independent variables are T, $c_1\cdots$, c_σ, and μ_w, the chemical potential of the solvent. The trans-

TABLE II. $\ln\gamma_\pm(\mathrm{HNC}_c)-\ln\gamma_\pm(\mathrm{HNC}_p)$.

c_2	$a_{++}=a_{--}=a_{+-}=4.6$ Å	$a_{++}=3.6$ Å, $a_{--}=5.6$ Å, $a_{+-}=4.6$ Å
0.1	0.0002	0.0007
0.2	0.0005	−0.0001
0.3	0.0008	0.0002
0.5[a]	0.001	0.001
0.7	0.000	0.000
0.8	0.000	−0.001
0.9	−0.001	−0.001
1.0	−0.002	−0.002

[a] The tabulated differences in $\ln\gamma_\pm$ for $c_2\geqq 0.5M$ are accurate to only ±0.001.

TABLE III. Results of the HNC equation for a 1–1 electrolyte in H_2O at 25°C.[a]

	$a_{++}=a_{--}=a_{+-}=4.6$ Å			$a_{++}=3.6$ Å, $a_{--}=5.6$ Å, $a_{+-}=4.6$ Å		
c_2	$d\ln\gamma_\pm/dc_2$	$\ln\gamma_\pm$	ϕ	$d\ln\gamma_\pm/dc_2$	$\ln\gamma_\pm$	ϕ
0.05	−1.043		0.9541	−1.020		0.9547
0.1	−0.4207	−0.2101	0.9530	−0.3936	−0.2072	0.9542
0.2	−0.0260	−0.2286	0.9641	+0.0049	−0.2237	0.9669
0.3	+0.1345	−0.2221	0.9818	0.1829	−0.2136	0.9865
0.5	0.2909	−0.1776	1.026	0.3249	−0.1604	1.035
0.7	0.3789	−0.1099	1.078	0.4220	−0.0848	1.092
0.8	0.4128	−0.0704	1.106	0.4615	−0.0407	1.124
0.9	0.4431	−0.0277	1.136	0.4957	+0.0071	1.156
1.0	0.4710	+0.0181	1.167	0.5269	+0.0583	1.191

[a] The tabulated values of $\ln\gamma_\pm$ have been obtained through the compressibility equation.

formations of the excess functions from such a system, which we may call the McMillan–Mayer system, to the conventional system, in which the independent variables are T, P, and the solute molalities, have been worked out[6] but here we shall only report values in the McMillan–Mayer system. For the system of charged hard spheres considered in this study, the expression for the excess pressure reduces to

$$P^{ex}=\frac{1}{6\epsilon}\sum_{i=1}^{\sigma}\sum_{j=1}^{\sigma}c_ic_je_ie_j\int_{a_{ij}}^{\infty}g_{ij}(r)4\pi r dr + \tfrac{1}{3}(2\pi kT)\sum_{i=1}^{\sigma}\sum_{j=1}^{\sigma}c_ic_jg_{ij}(a_{ij})a_{ij}^3, \quad (4.4)$$

in which the correlation functions $g_{ij}(a_{i,j})$ at the outer surface of contact are required. Using the multinomial theorem and the electroneutrality condition

$$\sum_{i=1}^{\sigma}\sum_{j=1}^{\sigma}c_ic_je_ie_j=\left(\sum_{i=1}^{\sigma}c_ie_i\right)^2=0, \quad (4.5)$$

the first term in Eq. (4.4) may be simplified further to obtain the final result

$$P^{ex}=\frac{1}{6\epsilon}\sum_{i=1}^{\sigma}\sum_{j=1}^{\sigma}c_ic_je_ie_jT_{ij} + \tfrac{1}{3}(2\pi kT)\sum_{i=1}^{\sigma}\sum_{j=1}^{\sigma}c_ic_jg_{ij}(a_{ij})a_{ij}^3, \quad (4.6)$$

where

$$T_{ij}\equiv -2\pi a_{ij}^2+4\pi\int_{a_{ij}}^{\infty}h_{ij}(r)r dr. \quad (4.7)$$

The generalization of Eq. (4.2) is shown in Appendix A to be

$$\nu(d\ln\gamma_\pm/dc_2)_{T,\mu_w}=\left[\frac{2\nu_+\nu_-G_{+-}+\nu_+^2G_{++}+\nu_-^2G_{--}+\nu_+\nu_-\nu c_2(G_{++}G_{--}-G_{+-}^2)}{1+c_2(\nu_+G_{++}+\nu_-G_{--})+\nu_+\nu_-c_2^2(G_{++}G_{--}-G_{+-}^2)}\right], \quad (4.8)$$

where we define $c_2\equiv c/\nu$ and

$$G_{ij}\equiv 4\pi\int_0^{\infty}h_{ij}(r)r^2dr. \quad (4.9)$$

Like other forms of the compressibility relation this equation does not depend on the direct potential being pairwise additive. The integrals G_{ij} and T_{ij} were determined numerically over the range up to $L=(N-1)\hat{r}$ by Simpson's rule, and the remainder evaluated analytically by assuming $h_{ij}=q_{ij}$ for $r>L$.

It is well known that the agreement of the thermodynamic functions computed from the correlation function by the pressure equation and the compressibility equation is a necessary condition for the accuracy of the correlation function. To employ this criterion we compute $\ln\gamma_\pm$ by each method as follows.

The function $d\ln\gamma_\pm/dc_2$ is computed from the compressibility equation from the results of a given integral equation with a given model at fourteen different concentrations, c_2=0.001, 0.002, 0.005, 0.007, 0.01, 0.02, 0.05, 0.1, 0.2, 0.3, 0.5, 0.7, 0.9, 1.0. These $d\ln\gamma_\pm/dc_2$ values are then compared with those obtained from the same model by the DHLL+B_2 approximation. The difference, call it $\Delta(c)$, is smooth and slowly varying and easily integrated. Then we have

$$\ln\gamma_\pm(c')=\{\text{DHLL}+B_2\}+\int_0^{c'}\Delta(c)dc, \quad (4.10)$$

where { } is the DHLL+B_2 contribution to $\ln\gamma_\pm(c')$. It is readily evaluated directly from the defining equations. This round-about method for integrating $d\ln\gamma_\pm/dc_2$ proves to be convenient because the singularity at $c=0$ does not appear and because not many values of $d\ln\gamma_\pm/dc_2$ are required for good accuracy.

Now from the same set of $g(r)$ functions used above we compute $\phi(c)$ by Eq. (4.6) to obtain $\ln\gamma_\pm(c')$ by integrating according to

$$d[c(1-\phi)]+cd\ln\gamma_\pm=0, \qquad (T \text{ and } \mu_w \text{ constant}) \tag{4.11}$$

which is an analogue of the Gibbs–Duhem equation that is useful for McMillan–Mayer systems or, of course, for gases. Again the integration is carried out by actually integrating only the difference between the integral equation value of ϕ and the DHLL+B_2 approximation to ϕ.

In Fig. 3 we show $\ln\gamma_\pm$ as a function of the square root of the molar ionic strength I. These functions have been computed by both methods from a given model using the HNC, PY, and $g(\Lambda)$ equations. It is apparent that the former is significantly superior by this criterion, and Table II confirms that in fact it leaves nothing to be desired. For this reason we also present in Table III the detailed results of the HNC equation; they serve as an accurate representation of the primitive model for the chosen set of parameters. We cannot be sure that the superiority of the HNC equation will persist as these methods are extended to a higher concentration range, different charge types, different short-range contributions to the potential, and to mixtures. But we can be sure that we can at last compute quite accurate values for the thermodynamic functions for the primitive model up to the molar concentration range.

TABLE IV. Study of the effect of the range of integration. System: All $a_{ij}=4.60$ Å, 1–1 electrolyte. Primitive model with the dielectric constant of water at 25°C. $\hat{r}\approx 0.015/\kappa$.

Molarity N	0.1		0.5	
	512	1024	512	1024
Results from $g_{ij}(\Lambda)$				
$d\ln\gamma_\pm/dc_2$	−0.4248	−0.4247	0.3019	0.3019
ϕ	0.9495	0.9497	1.013	1.012
Results after iteration (HNC equation)				
$G_{++}/10^4$	−0.7923	−0.7912		
$G_{+-}/10^4$	0.8652	0.8641		
$H_{++}/10^2$ [a]	−0.5104	−0.5103		
$H_{+-}/10^2$	0.4562	0.4561		
$d\ln\gamma_\pm/dc_2$	−0.4207	−0.4205		
ϕ	0.9530	0.9530		

[a] $H_{ij}\equiv T_{ij}/4\pi$.

V. RESULTS AND DISCUSSION

At this stage we should again recall the approximations that were listed at the end of Sec. III. They are all difficult to assess by analytical methods but the numerical tests that we have made all tend to show that these approximations, separately and collectively, are not important in the computations we have completed. The most impressive evidence for this is the accurate agreement of the $\ln\gamma_\pm$ functions calculated from the HNC equation via the pressure equation and

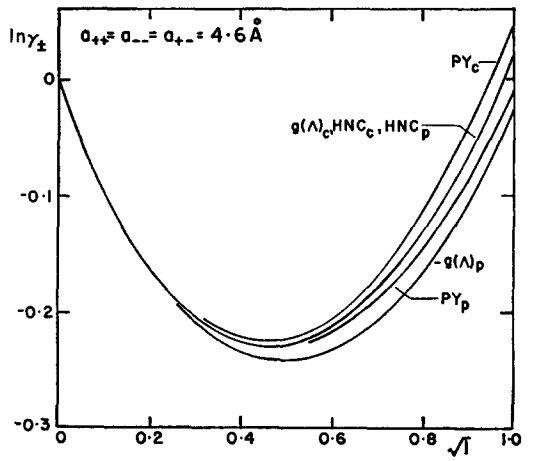

FIG. 3. $\ln\gamma_\pm$ functions obtained by alternative integration of the correlation functions; curves marked c were obtained by the compressibility equation and the curves marked p were obtained by the pressure equation.

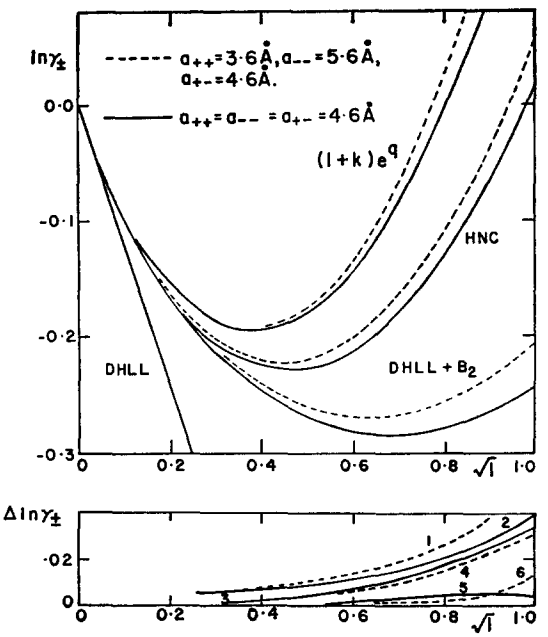

FIG. 4. $\ln\gamma_+$ functions from the HNC equation compared with several other approximations for two sets of ionic parameters. Except for DHLL+B_2, all of these results have been obtained by applying the compressibility equation. The ordinate of the lower graph has a scale twice that of the upper one, and the curves have been calculated as follows:

1 and 2	HNC–$w(\Lambda)$,
3 and 4	PY–HNC,
5	$g(\Lambda)$–HNC,
6	HNC–$g(\Lambda)$.

TABLE V. Comparison of present calculations with those of Carley.

				ϕ by HNC		ϕ by PY	
σ	a	θ	m/molar	Carley	Present work	Carley	Present work
0.4	11.5	1.61	0.261	0.976	0.974	0.965	0.972
0.6	7.66	1.07	0.806	1.12	1.14	1.13	1.12

the compressibility equation as cited in Sec. IV. Still we have not yet carried out this test for many systems and it may be suspected that the accurate agreement results from a fortuitous cancellation of errors. For this reason we have made an independent check by repeating one HNC calculation with the same $\hat{r}$ as used earlier but with $N=1024$ rather than 512. This was done on another IBM 7044 computer that has a much larger core memory.[16] The comparison summarized in Table IV shows that the independence of N for these cases is systematic and so cannot reflect a fortuitous cancellation.

In Fig. 4 we compare $\ln\gamma_{\pm}$ as calculated by the HNC equation with several other approximations, all for two sets of a_{ij} parameters. All of these have been obtained by the compressibility equation. It is striking that the $g(\Lambda)$ approximation, which is defined in Eq. (2.16) and which serves as the trial function in all of our iterative procedures, gives a result which is so close to the HNC result so that for many purposes there is no point in solving the integral equation. This point is emphasized by Fig. 5 in which we make the same comparison for the osmotic coefficients. All of these have been obtained by the pressure equation and this should be borne in mind if one is tempted to interpret the differences in order in the two graphs. The approximations $g(\Lambda)$ and $\omega(\Lambda)$ are more sensitive than the PY equation to the choice of the compressibility equation or pressure equation method of integrating the distribution functions. But the dominant feature is the accuracy of the $g(\Lambda)$ approximation which must be interpreted as resulting from a widespread cancellation of higher terms. This is reminiscent of the cancellation found when the PY equation is applied to fluids composed of hard spheres without charges. Another approximation is Eq. (2.14), the results of which are labelled $(1+k)e^q$ in Figs. 4 and 5. This equates the potential of average force to the sum of the short-range potential (u^*) and the Debye screened potential (kTq), but overestimates the corrections to the Debye–Hückel limiting law, while the $w(\Lambda)$ approximation which retains in addition the next term in the potential of average force underestimates the corrections to the limiting law. Thus we find that the $\ln\gamma_{\pm}$ and ϕ functions for the approximations $(1+k)e^q$ and $w(\Lambda)$ lie on either side of the corresponding functions for the HNC approximation which we have shown to be the most accurate of the five approximations studied by us.

The effect of changing the a_{++} and a_{--} parameters to be different from the a_{+-} parameter is shown in Fig. 6. Obviously many more comparisons of this kind could be made; we only demonstrate here that the effect of this change is sizeable but does not dominate the picture.

It is of interest to compare these results with those of Carley who employed the HNC and PY equations (without prior summation of the chains) which have been derived for more general intermolecular potentials. He also used different numerical procedures from ours in applying them to electrolyte solutions. These equations are different from their analogs, derived by Allnatt for the particular case of ionic systems, but the two HNC approximations are equivalent and should give identical results.[1] Unfortunately the range of overlap of his calculations with the region of most interest here is not large. However, we have been able to compare two systems as shown in Table V where the parameters are those derived by Carley. The agreement between the HNC results is all that one can expect for these systems (for which all $a_{ij}=4.60$ Å) since we had to interpolate or slightly extrapolate his results. The results for the two PY approximations indicate that, though they are not theoretically equivalent, the difference between them is small.

Considerable work is required before a systematic comparison of the primitive model results with experiment will be in hand; the corrections to the McMillan–Mayer standard states from the conventional standard states[6] have to be worked out for each system and the calculations here have to be repeated for many sets of ion size parameters. However, a preliminary comparison shown in Fig. 7 indicates that these results may be quite interesting. The DHLL+B_2 curve is known to fall quite close to the extended form of the Debye–Hückel limiting law which many authors have chosen to represent the primitive model. Proceeding on this assumption Stokes and Robinson interpreted the difference between this and the experimental curve for LiBr as due to "hydration," worked out a theory for this, and derived a hydration number. We see however that the true primitive model function for the same ion size parameter falls *above* the experimental curve, so their result is without any basis. It remains to be seen whether the primitive model curve which

[16] We thank Dr. H. Freitag for arranging the use of the computer at the IBM Laboratory, Yorktown Heights, New York.

best fits these LiBr data will curve upward more or less sharply than the data.

APPENDIX A. GENERALIZATION OF THE COMPRESSIBILITY EQUATION FOR IONIC SOLUTIONS

This calculation follows the method used by Kirkwood and Buff[17] for a similar problem but is developed with the restraints of the solution of a single electrolyte

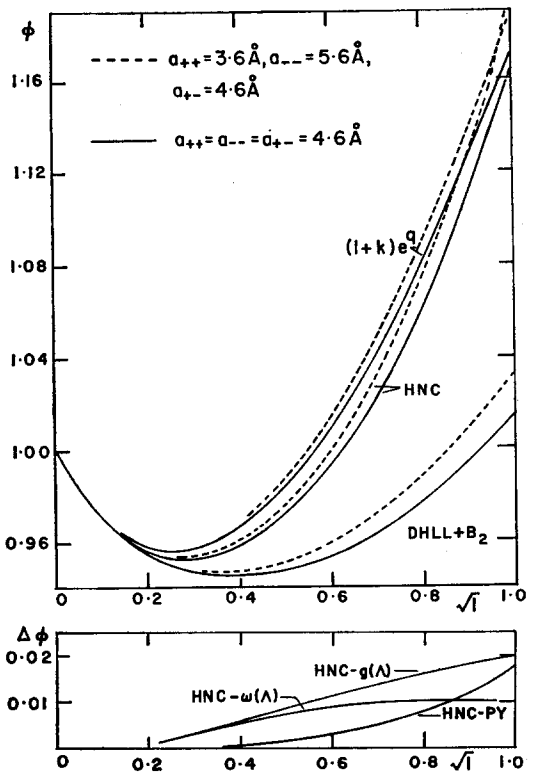

FIG. 5. Comparison of the osmotic coefficients obtained from various approximations. The parameters are the same as in Fig. 4 but here the pressure equation has been used in calculating ϕ from the correlation functions. The ordinate of the lower graph has a scale twice that of the upper one, and the curves are identical for both sets of ionic parameters.

in mind. In this Appendix the solvent is denoted by subscript 1, the solute by subscript 2, and the ionic components are variously i, j, or k.

The composition fluctuations in the grand ensemble give the relations

$$kT(\partial N_i/\partial\mu_j)_{T,\mu_1,\mu_k}=kT(\partial N_j/\partial\mu_i)_{T,\mu_1,\mu_k}$$
$$=\langle N_iN_j\rangle-\langle N_i\rangle\langle N_j\rangle, \quad \text{(A1)}$$

where the subscript μ_k means all ionic μ's except the one indicated in the differentiation. The definition of g_{ij} in the grand ensemble and the assumption of spherical symmetry for these correlation functions gives

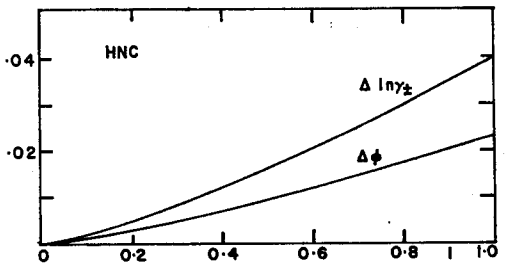

FIG. 6. Differences in $\ln\gamma_\pm$ and ϕ for two sets of ionic parameters in the HNC equation; the effects of $a_{++}\neq a_{--}\neq a_{+-}$. Here $\Delta x\equiv x(a_{++}=3.6$ Å, $a_{--}=5.6$ Å, $a_{+-}=4.6$ Å$)-x($all $a_{ij}=4.6$ Å$)$.

$$c_ic_j\int_V(g_{ij}-1)d^3r_id^3r_j=c_ic_jV4\pi\int_0^\infty(g_{ij}-1)r_{ij}^2dr_{ij}$$
$$=\langle N_iN_j\rangle-\langle N_i\rangle\langle N_j\rangle-Vc_j\delta_{ij}. \quad \text{(A2)}$$

Defining G_{ij} by Eq. (4.5) one obtains from the above equations the important relation

$$M_{ij}\equiv(\partial c_i/\partial\mu_j)_{T,\mu_1,\mu_k}$$
$$=(\partial c_j/\partial\mu_i)_{T,\mu_1,\mu_k}$$
$$=(kT)^{-1}(c_ic_jG_{ij}+c_j\delta_{ij}). \quad \text{(A3)}$$

This perfectly general equation may also be obtained from the McMillan–Mayer theory.

Assuming that there are σ ionic species in solution, there are σ components each for the vectors $\boldsymbol{\mu}$ and $\mathbf{c}$ representing the chemical potentials and concentrations, respectively, of the ions, and σ^2 elements M_{ij} in the square matrix $\mathbf{M}$ which is symmetric. Hence for the McMillan–Mayer system (T and μ_1 constant) we have the set of equations

$$d\mathbf{c}=\mathbf{M}d\boldsymbol{\mu}. \quad \text{(A4)}$$

To transform from the variables (T,μ_1,μ_k) to (T,μ_1,c_k)

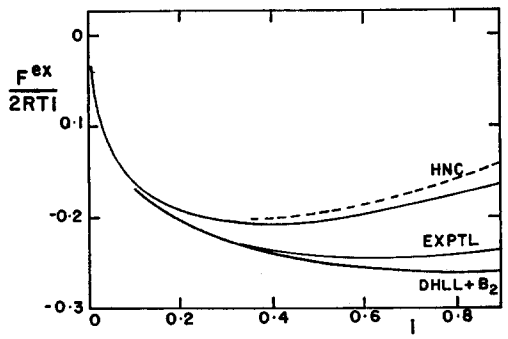

FIG. 7. $F^{ex}/2RTI$ from the HNC and (DHLL+B_2) approximations compared with the experimental values for LiBr in H_2O at 25°C. Two sets of HNC curves are shown: —— all $a_{ij}=4.6$ Å; – – – $a_{++}=3.6$ A, $a_{+-}=4.6$ Å, $a_{--}=5.6$ Å. The experimental values have been corrected from the conventional standard states to the McMillian–Mayer standard states.

[17] J. G. Kirkwood and F. P. Buff, J. Chem. Phys. **19**, 774 (1951).

we merely invert Eq. (A4) to obtain the set

$$d\mu = \mathsf{M}^{-1} d\mathbf{c},$$
$$(\mathsf{M}^{-1})_{ij} = \text{cofactor of } M_{ji}/\det\mathsf{M}, \qquad \text{(A5)}$$

which also applies to the ions in the same McMillan–Mayer system. In particular, for the solution of a single electrolyte, if

$$\mathsf{M} = \begin{bmatrix} M_{++} & M_{+-} \\ M_{-+} & M_{--} \end{bmatrix},$$

then

$$\mathsf{M}^{-1} = \frac{\begin{bmatrix} M_{--} & -M_{+-} \\ -M_{-+} & M_{++} \end{bmatrix}}{\det\mathsf{M}}, \qquad \text{(A6)}$$

where

$$\det\mathsf{M} = [c_+c_-/(kT)^2][1 + c_+G_{++} + c_-G_{--} + c_+c_-(G_{++}G_{--} - G_{+-}^2)]. \qquad \text{(A7)}$$

From Eqs. (A3), (A5), and (A6) and the following definitions

$$d\mu_2 \equiv \nu_+ d\mu_+ + \nu_- d\mu_- \qquad T \text{ and } \mu_1 \text{ constant}$$
$$c_+ \equiv \nu_+ c_2, \qquad c_- \equiv \nu_- c_2 \qquad \nu \equiv \nu_+ + \nu_-$$

one obtains

$$kT(\partial\mu_2/\partial c_2)_{T,\mu_1} = \nu_+\nu_-[\nu c_2 + c_+c_-(G_{++} + G_{--} - 2G_{+-})]/\det\mathsf{M}. \qquad \text{(A8)}$$

Equation (A8) reduces to Eq. (19) in Kirkwood and Buff's paper,[17] in the limit

$$G_{++} = G_{--} = G_{+-} \equiv G_{22},$$

with the use of the relation

$$c_2 d\mu_2 - dP = 0,$$

which applies at constant T and μ_1. On removing the ideal contribution from Eq. (A8), the expression given in Eq. (4.4) for the nonideal term $(d\ \ln\gamma_\pm/dc_2)_{T,\mu_1}$ is obtained. Equation (4.4) gives the Debye–Hückel limiting law asymptotically in the limit of infinite dilution, when the leading term, $(1+k_{ij})\exp(q_{ij})$, in the correlation function $g_{ij}(r)$ is substituted in the expression for G_{ij}, and the exponential expanded as far as the first three terms.

ACKNOWLEDGMENTS

We are grateful to Dr. R. L. Garwin of IBM for informing us about the fast Fourier transform procedure which made this work possible, to Dr. J. W. Cooley of IBM for assistance with the subroutine FORT, and to Dr. H. Freitag of IBM for the use of the computer facilities at Yorktown Heights for a test which requires a computer with an exceptionally large core memory. We acknowledge the donation of computing time by the Computing Center of this university, and thank members of the staff, Mr. Herbert Hopf and Dr. David Levine, for assistance with the program. We also thank Anthea R. Rasaiah for extensive clerical assistance with the computation.

THE JOURNAL OF CHEMICAL PHYSICS VOLUME 48, NUMBER 6 15 MARCH 1968

Spin Degeneracy in the AMO Method. Excited States of the Benzene Molecule*

STEN LUNELL AND PETER LINDNER
Quantum Chemistry Group for Research in Atomic, Molecular, and Solid State Theory, Uppsala University, Uppsala, Sweden
(Received 29 September 1967)

The spin-degeneracy problem in the alternant molecular-orbital (AMO) method, as applied to excited states of the benzene molecule, is investigated. The results obtained using the full nine-dimensional triplet spin space and the five-dimensional quintet space show in the one-parameter method an energy improvement over the ones obtained by a conventional AMO treatment of 0.659 eV for the $^3B_{1u}$ state and 0.975 eV for the $^5A_{1g}$ state. When two mixing parameters are used the corresponding improvements are much smaller, 0.029 eV and 0.032 eV, respectively. Results are also presented for some additional states, not occurring in the ordinary AMO method.

INTRODUCTION

The alternant molecular orbital (AMO) method was proposed by Löwdin[1] in order to remove some of the correlation error attached to the conventional MO–LCAO scheme. A detailed description of the method can be found in a series of papers by Löwdin, Pauncz, and de Heer[2] and in a newly published book by Pauncz,[3] so that only a brief outline is given below.

* The research reported in this document has been sponsored in part by the Air Force Office of Scientific Research (OSR), through the European Office of Aerospace Research (OAR) United States Air Force, under Contract AF 61(052)-874.

[1] P.-O. Löwdin, Symp. Mol. Phys., Nikko, Japan, 1953, 13 (1954).

[2] (a) P.-O. Löwdin, Phys. Rev. **97**, 1509 (1955); (b) R. Pauncz, J. de Heer, and P.-O. Löwdin, J. Chem. Phys. **36**, 2247, 2257 (1962); (c) J. de Heer, J. Phys. Chem. **66**, 2288 (1962); (d) R. Pauncz, J. Chem. Phys. **37**, 2739 (1963); (e) J. de Heer and R. Pauncz, *ibid.* **39**, 2314 (1963).

[3] R. Pauncz, *Alternant Molecular Orbital Method* (W. B. Saunders Co., Philadelphia, Pa., 1967).